Synthesis of Atomically Precise Single-Crystalline Ru_2-Based Coordination Polymers

Wen-Yang Gao, Gerard Pierre Van Trieste III, and David C. Powers*

Texas A&M University, 3255 TAMU, College Station, TX 77843, United States

ABSTRACT Methods to incorporate kinetically inert metal nodes and highly basic ligands into single-crystalline metal-organic frameworks (MOFs) are scarce, which prevents synthesis and systematic variation of many potential heterogeneous catalyst materials. Here we demonstrate that metallopolymerization of kinetically inert Ru_2 metallomonomers via labile Ag–N bonds provides access to a family of atomically precise single-crystalline Ru_2-based coordination polymers with varied network topology and primary coordination sphere.

Metal-organic frameworks (MOFs) have attracted significant attention as platforms for heterogeneous catalysis in part due to the diversity of metal geometries and cluster sizes that can be incorporated within the extended crystal lattices of these materials.[1,2] Reticular synthetic logic enables systematic variation of structural parameters during MOF synthesis.[3-6] While access to single-crystalline materials facilitates characterization of catalyst structure,[7] observation of reactive species,[8-10] and systematic modulation of substrate diffusivity,[11-15] obtaining single-crystalline materials requires that the lattice be constructed via reversible metal–ligand bond formation. As a result, it is challenging to incorporate kinetically inert metal ions into highly crystalline materials.[16,17] A less appreciated ramification of the need for reversible M–L bonding is that the primary coordination sphere of lattice ions is frequently limited to weak-field donors, which can engage in rapid exchange.[18] In contrast, a much wider variety of ligand donicities are routinely utilized in homogeneous catalysis.[19-23] Development of methods that enable systematic variation of the primary coordination sphere of lattice ions are needed to access the full array of potential MOF catalysts.

We have been interested in Ru_2-based MOFs as platforms for nitrogen-atom and nitrene-transfer catalysis.[15,24-26] Due to the slow ligand exchange kinetics characteristic of Ru^{2+} and Ru^{3+}, the family of available Ru_2-based MOFs is extremely limited: Only $[Ru_6(btc)_4Cl_3]$ is available from solvothermal methods and only as a microcrystalline powder (btc = 1,3,5-benzenetricarboxylate).[27,28] To provide access to new Ru_2-based materials, we have been developing metallopolymerization chemistry in which pre-synthesized metallomonomers featuring peripheral functionality are polymerized under conditions in which the metallomonomers are kinetically stable (Figure 1).[25,29] The metallopolymerization strategy enables systematic variation of both network topology and the primary coordination sphere of lattice ions by rational perturbation of the molecular structure of the constituent metallomonomers. We previously demonstrated metallopolymerization via Sonogashira coupling of halogenated Ru_2 complexes with polyalkynes (Figure 1a)[25] and via mechanochemical reaction of carboxylated Ru_2 complexes with the $Cu(OAc)_2$ salt provided amorphous and microcrystalline porous solids, respectively (Figure 1b).[29] In neither case were single-crystalline

materials available. Inspired by classic reports of coordination polymers based on Ag–nitrile linkages,[30-33] here we report the metallopolymerization of a family of Ru_2 complexes featuring peripheral nitrile substituents with Ag^+. This synthetic strategy provides access to a family of single-crystalline Ru_2-based materials, in which both network topology and primary coordination sphere of lattice ions can be systematically manipulated (Figure 1c).

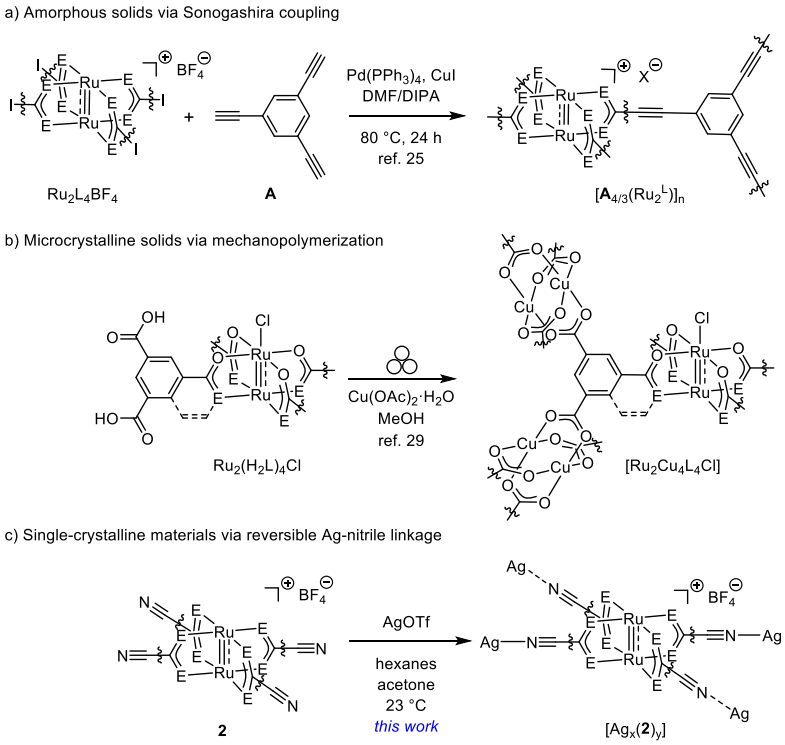

Figure 1. Previous metallopolymerization chemistry based on a) Sonogashira coupling reaction of halogenated Ru_2 complexes with polyalkynes or b) mechanopolymerization synthesis of carboxylated Ru_2 complexes with $Cu(OAc)_2$ resulted in amorphous solids or microcrystalline powders, respectively. c) Here, we report the synthesis of single-crystalline heterobimetallic materials based on systematically variable kinetically inert metallomonomers and reversibly generated Ag-nitrile linkages.

We initiated these investigations by preparing a family of Ru_2[II,III] complexes (**2**, Figure 2) featuring peripheral nitrile groups in which both the substitution pattern (*i.e.*, 3- *vs.* 4-monosubstitution and 3,5-disubstitution) and the primary coordination sphere (*i.e.* carboxylate, 2-oxypyridinate, and 2-aminopyridinate) were varied. These metallomonomers were synthesized by thermally promoted ligand exchange between $Ru_2(OAc)_4Cl$ and the appropriate ligand. Ligand exchange was monitored by mass spectrometry (*i.e. m*/*z* value that corresponded to $[Ru_2L_4]^+$) and ^{1}H NMR spectroscopy. The ^{1}H NMR spectra of **2a**, **2b**, and **2c** display the appropriate number of paramagnetically shifted signals, which is similar to the ^{1}H NMR data obtained for $Ru_2(OBz)_4Cl$. Neither 2-aminopyrdinate- nor 2-oxypyridinate- based Ru_2L_4Cl complexes (**2d** and **2e**) display well-defined ^{1}H NMR signals when measured in d_6-DMSO at 295 K, which is similar to ^{1}H NMR data of iodinated analogues.[25] Ru_2L_4Cl complexes often display poor solubility due to the formation of $[–Ru–Ru–Cl–]_n$ chains,[25,34,35] and consistent with this, complexes **1** display poor solubility in many common solvents. Treatment of complexes **1** with $AgBF_4$ afforded $[Ru_2L_4]BF_4$ complexes **2**, which displayed significantly enhanced solubility. The anion exchange process was

characterized by the appearance of a broad B–F IR stretching mode at 1020 cm^{-1} (Figures S1–S5). The molecular structure of $Ru_2(4\text{-CN-OBz})_4BF_4$ (**2a**) was established by single-crystal X-ray diffraction (SCXRD, Figure S6).

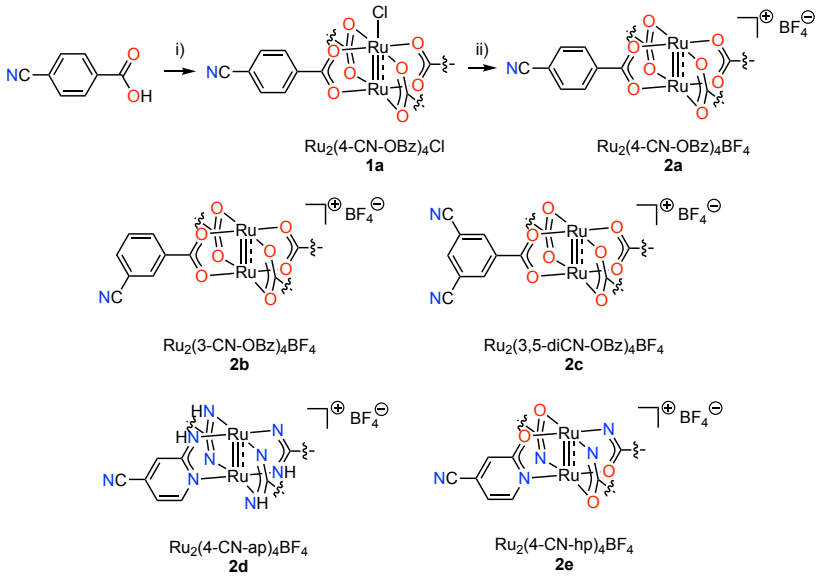

Figure 2. A two-step synthetic procedure based on ligand exchange followed by anion exchange, affords a family of soluble metallomonomers (**2**). Conditions: i) **1a**–**1b**: MeOH/H_2O, 90 °C; **1c**: PhCl, 150 °C, 14 h; **1d**–**1e**: PhCl, 155 °C, 24 h. ii) **2a**–**2b**: MeOH, 23 °C, 24 h; **2c**: THF, 23 °C, 24 h; **2d**: THF, 23 °C, 24 h; **2e**: MeOH, 65 °C, 24 h. THF = tetrahydrofuran, ap = aminopyridinate, hp = hydroxypyridinate.

With access to a suite of soluble Ru_2 complexes featuring peripheral nitrile substituents, we investigated metallopolymerization chemistry in the presence of silver trifluoromethanesulfonate (AgOTf). Diffusion of hexanes into a solution of $Ru_2(4\text{-CN-OBz})_4BF_4$ (**2a**) and AgOTf in acetone afforded orange-colored block-shaped crystals (Figure 3a). SCXRD analysis revealed a two-dimensional (2D) layered structure in which there are two different coordination modes for metallomonomers incorporated into the framework: one metallomonomer is coordinated to four Ag(I) nodes via each of the nitrile substituents while the other metallomonomer is coordinated to two Ag(I) nodes via trans-disposed nitriles (the other two nitriles are not coordinated to Ag(I); Figure 3b). Each Ag(I) ion in the coordination polymer is trigonally coordinated with an average Ag–N distance of 2.06 Å and the average N–Ag–N angle 111.7°. The extended 2D layer (Figure S7) is singly interpenetrated by another layer (Figure 3c). Attempts to generate this structure by solvothermal combination of 4-cyanobenzoic acid, $Ru_2(OAc)_4Cl$, and AgOTf were unsuccessful due to formation of Ag mirror.[36]

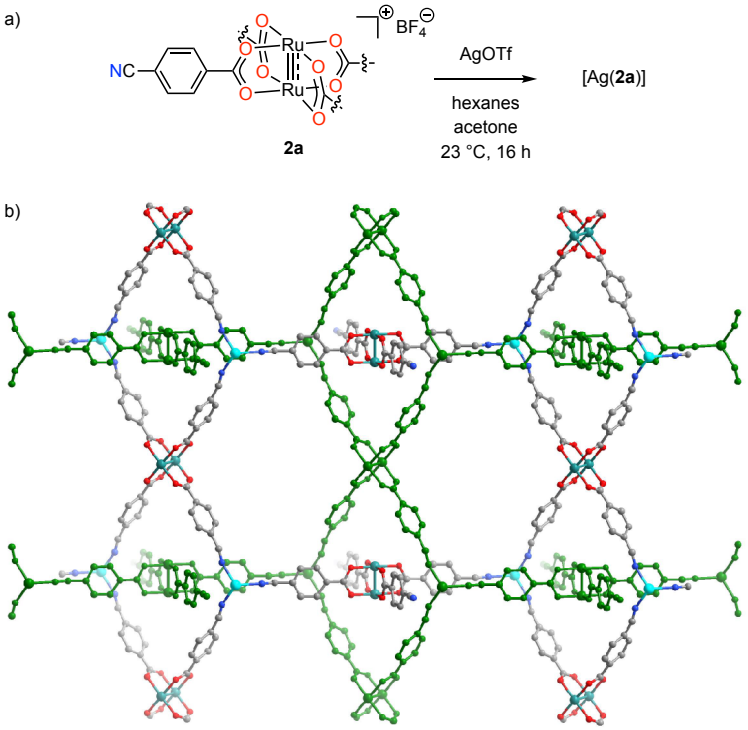

Figure 3. a) Diffusion of hexanes into an acetone solution of Ru_2(4-CN-OBz)$_4BF_4$ (**2a**) and AgOTf affords orange-colored block-shaped crystals of [Ag(**2a**)]. b) A two-dimensional extended coordination polymer of [Ag(**2a**)] was revealed by SCXRD. The second interpenetrated layer is marked green.

Moving the position of nitrile substituent from 4- to 3- on the metallomonomer (*i.e.* **2b**) changes the resultant structure from two-fold interpenetrated 2-D sheets to self-assembled 1-D chains. A crystallization reaction between Ru_2(3-CN-OBz)$_4BF_4$ (**2b**) and AgOTf afforded a solid in which each Ag(I) ion is two-coordinate, bound to nitrogens of two nitrile groups at distances of 2.11(2) and 2.18(2) Å with a N–Ag–N angle of 151.5(6)° (Figure 4a). The nitrile ligands display pairwise directionality, with two *cis*-disposed nitrile pointing up and the other two *cis*-disposed nitriles pointing down. This alternating directionality gives rise to the infinite double-chain structure illustrated in Figure 4b.

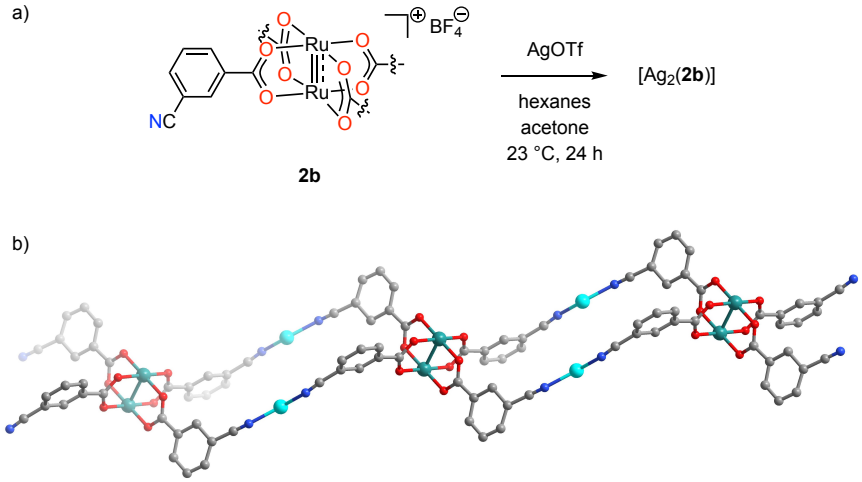

Figure 4. a) Diffusion of hexanes into an acetone solution of Ru_2(3-CN-OBz)$_4BF_4$ (**2b**) and AgOTf affords orange-colored crystals of [Ag_2(**2b**)]. b) Pairwise directionality of the nitrile substituents gives rise to the observed double-chain structure.

An extended 3-D network was accessed by expanding the connectivity of the metallomonomer from 4 to 8 (*i.e.*, utilized metallomonomer **2c** in place of **2a** or **2b**). Metallopolymerization of Ru_2(3,5-diCN-OBz)$_4BF_4$ (**2c**) with AgOTf afforded dark orange single crystals (Figure 5a). SCXRD analysis of [Ag_2(**2c**)] revealed a two-fold interpenetrated 3-D network. Two types of Ag(I) nodes were observed in this structure: one Ag(I) node is trigonally coordinated by three nitriles; the other Ag(I) adopts tetrahedral coordination geometry with four nitriles. There are two distinct metallomonomer connectivities: one metallomonomer is coordinated to Ag(I) via all eight nitriles (see Figure 5b left); the other metallomonomer is coordinated to Ag(I) via four nitriles (one from each 3,5-dicyanobenzoate motif, see Figure 5b right). This results to an expanded 3-D network (Figure 5c), which is interpenetrated by another network (Figure S8).

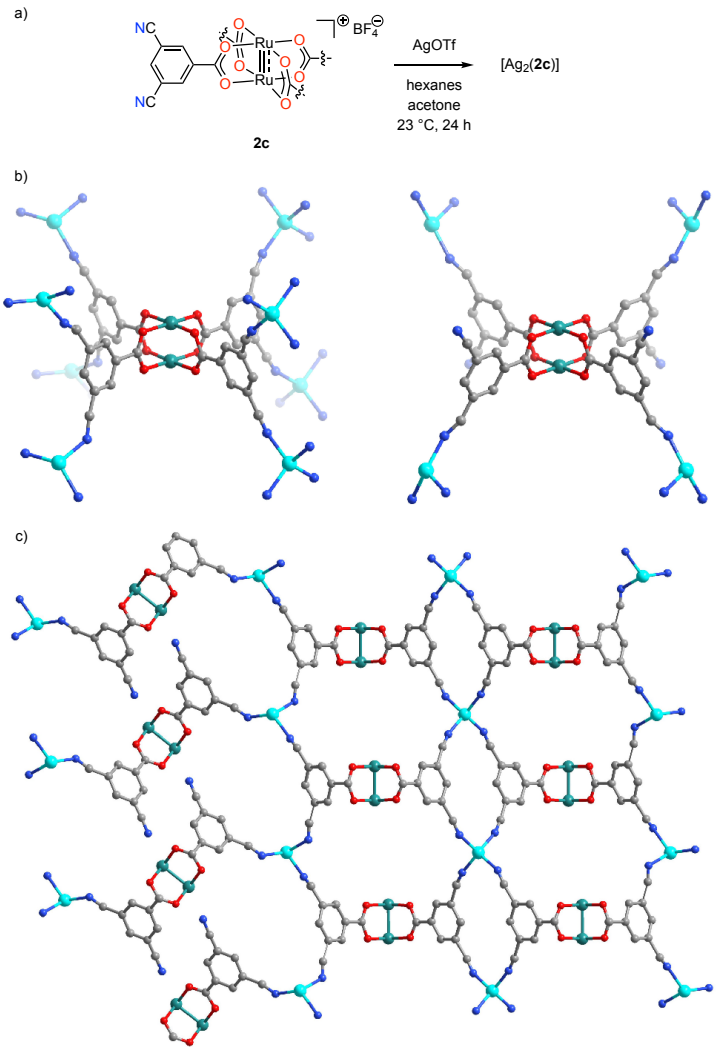

Figure 5. a) Diffusion of hexanes into an acetone solution of Ru_2(3,5-diCN-OBz)$_4BF_4$ (**2c**) and AgOTf affords dark orange-colored crystals of [Ag_2(**2c**)]. b) A three-dimensional extended coordination polymer was revealed by SCXRD Two types of Ag(I) nodes and two kinds of the metallomonomers are observed in the structure. c) An extended network is viewed from *b* axis without the interpenetrating net. The non-coordinated nitrile groups are visible in this direction

The modularity of the developed metallopolymerization strategy enables systematic variation of the primary coordination sphere of lattice-confined Ru_2 sites within single-crystalline materials. Metallopolymerization of Ru_2(4-CN-ap)$_4BF_4$ (**2d**) with AgOTf affords a 2-D sheet in which each nitrile of the metallomonomer is linearly coordinated Ag(I) nodes (Figure S9). Metallopolymerization of Ru_2(4-CN-hp)$_4BF_4$ (**2e**) with AgOTf affords an extended material comprised of 3-D networks (Figure S10). The 3-D connectivity in this case arises from axial binding of a hydroxypyridine ligand to the apical site of the Ru_2 node, thus affording the dimensionally expanded network.

Powder X-ray diffraction (PXRD) analysis of the developed materials [Ag_x(**2**)$_y$] reveals the family of polymers to be sensitive to desolvation. While the facility of Ag–nitrile reversibility provides

access to single-crystalline materials, desolvation results in network collapse and amorphization (see Figure S11 for PXRD). These observations are consistent with previous reports of Ag nitrile-based coordination polymers,[37-40] and highlights a critical design challenge for the development of broadly useful metallopolymerization chemistry: A delicate balance between the requirement for strong M–L linkages to provide network stability to the resulting materials while simultaneously having sufficient M–L lability to access single-crystalline materials.

In summary, we describe a synthetic strategy to incorporate kinetically inert Ru_2 nodes into single-crystalline coordination polymers, which takes advantages of the facile Ag–N bond formation between nitrile groups of metallomonomers and Ag(I) under self-assembly conditions. By modulating the geometry and connectivity of the metallomonomers, the resultant structures can be varied from 1-D chains to 2-D sheets and 3-D networks. The modularity of the metallopolymerization strategy enables the primary coordination sphere of lattice-bound Ru_2 nodes to be systematically varied within single-crystalline, atomically precise materials. We expect that further development of metallopolymerization concepts will result in new opportunities to rationally access robust catalyst platforms.

Corresponding Author
powers@chem.tamu.edu

Acknowledgement
This research was supported by the U.S. Department of Energy, Office of Science, Office of Basic Energy Sciences, Catalysis program, under award DE-SC0018977. The authors additionally thank The Welch Foundation (A-1907) for supporting preliminary experimental work. We thank Yu-Sheng Chen for acquisition of sing-crystal X-ray diffraction data of [Ag_2(**2c**)]. NSF's ChemMatCARS Sector 15 is principally supported by the Divisions of Chemistry (CHE) and Materials Research (DMR), National Science Foundation, under grant number NSF/CHE-13834750. Use of the Advanced Photon Source, an Office of Science User Facility operated for the U.S. Department of Energy (DOE) Office of Science by Argonne National Laboratory, was supported by the U.S. DOE under Contract No. DE-AC02-06CH11357.

References

1 J. R. Bour, A. M. Wright, X. He and M. Dincă, *Chem. Sci.*, 2020, **11**, 1728–1737.
2 A. Dhakshinamoorthy, Z. Li and H. Garcia, *Chem. Soc. Rev.*, 2018, **47**, 8134–8172.
3 O. M. Yaghi, *J. Am. Chem. Soc.*, 2016, **138**, 15507–15509.
4 S. Kitagawa, R. Kitaura and S.-i. Noro, *Angew. Chem. Int. Ed.*, 2004, **43**, 2334–2375.
5 R. Robson, *Dalton Trans.*, 2008, 5113–5131.
6 B. F. Hoskins and R. Robson, *J. Am. Chem. Soc.*, 1990, **112**, 1546–1554.
7 V. Pascanu, G. G. Miera, A. K. Inge and B. Martín-Matute, *J. Am. Chem. Soc.*, 2019, **141**, 7223–7234.
8 A. Das, G. P. III. Van Trieste and D. C. Powers, *Comm. Inorg. Chem.*, 2020, **40**, 116–158.
9 R. J. Young, M. T. Huxley, E. Pardo, N. R. Champness, C. J. Sumby and C. J. Doonan, *Chem. Sci.*, 2020, **11**, 4031–4050.
10 S. D. Pike and A. S. Weller, *Philos. Trans. R. Soc. A*, 2015, **373**, 20140187.
11 W.-Y. Gao, A. D. Cardenal, C.-H. Wang and D. C. Powers, *Chem. Eur. J.*, 2019, **25**, 3465–3476.

12 T. M. Tovar, J. Zhao, W. T. Nunn, H. F. Barton, G. W. Peterson, G. N. Parsons and M. D. LeVan, *J. Am. Chem. Soc.*, 2016, **138**, 11449–11452.
13 J.-P. Zhang, A.-X. Zhu and X.-M. Chen, *Chem. Commun.*, 2012, **48**, 11395–11397.
14 F. Song, C. Wang, J. M. Falkowski, L. Ma and W. Lin, *J. Am. Chem. Soc.*, 2010, **132**, 15390–15398.
15 C.-H. Wang, W.-Y. Gao and D. C. Powers, *J. Am. Chem. Soc.*, 2019, **141**, 19203–19207.
16 X. Lian, D. Feng, Y.-P. Chen, T.-F. Liu, X. Wang and H.-C. Zhou, *Chem. Sci.*, 2015, **6**, 7044–7048.
17 Notable exceptions are Cr(III)-based MIL-100, MIL-101, which have been obtained only as microcrystalline powders. See a) G. Férey, C. Serre, C. Mellot-Draznieks, F. Millange, S. Surblé, J. Dutour and I. Margiolaki, *Angew. Chem. Int. Ed.*, 2004, **43**, 6296–6301; b) G. Férey, C. Mellot-Draznieks, C. Serre, F. Millange, J. Dutour, S. Surblé and I. Margiolaki, *Science*, 2005, **309**, 2040–2042.
18 C. H. Hendon, A. J. Rieth, M. D. Korzyński and M. Dincă, *ACS Cent. Sci.*, 2017, **3**, 554–563.
19 C. Yoo, H. M. Dodge and A. J. M. Miller, *Chem. Commun.*, 2019, **55**, 5047–5059.
20 T. A. Jackson, J.-U. Rohde, M. S. Seo, C. V. Sastri, R. DeHont, A. Stubna, T. Ohta, T. Kitagawa, E. Münck, W. Nam and L. Que, Jr., *J. Am. Chem. Soc.*, 2008, **130**, 12394–12407.
21 J. Annaraj, J. Cho, Y.-M. Lee, S. Y. Kim, R. Latifi, S. P. de Visser and W. Nam, *Angew. Chem. Int. Ed.*, 2009, **48**, 4150–4153.
22 H. Suzuki, K. Inabe, Y. Shirakawa, N. Umezawa, N. Kato and T. Higuchi, *Inorg. Chem.*, 2017, **56**, 4245–4248.
23 M. E. Crestoni, S. Fornarini and F. Lanucara, *Chem. Eur. J.*, 2009, **15**, 7863–7866.
24 C.-H. Wang, A. Das, W.-Y. Gao and D. C. Powers, *Angew. Chem. Int. Ed.*, 2018, **57**, 3676–3681.
25 W.-Y. Gao, A. A. Ezazi, C.-H. Wang, J. Moon, C. Abney, J. Wright and D. C. Powers, *Organometallics*, 2019, **38**, 3436–3443.
26 A. Das, J. H. Reibenspies, Y.-S. Chen and D. C. Powers, *J. Am. Chem. Soc.*, 2017, **139**, 2912–2915.
27 O. Kozachuk, K. Yusenko, H. Noei, Y. Wang, S. Walleck, T. Glaser and R. A. Fischer, *Chem. Commun.*, 2011, **47**, 8509–8511.
28 C. R. Wade and M. Dincă, *Dalton Trans.*, 2012, **41**, 7931–7938.
29 W.-Y. Gao, A. Sur, C.-H. Wang, G. R. Lorzing, A. M. Antonio, G. A. Taggart, A. A. Ezazi, N. Bhuvanesh, E. D. Bloch and D. C. Powers, *Angew. Chem. Int. Ed.*, 2020, **59**, 10878–10883.
30 G. B. Gardner, D. Venkataraman, J. S. Moore and S. Lee, *Nature*, 1995, **374**, 792–795.
31 K. A. Hirsch, D. Venkataraman, S. R. Wilson, J. S. Moore and S. Lee, *J. Chem. Soc., Chem. Commun.*, 1995, 2199–2200.
32 K. A. Hirsch, S. R. Wilson and J. S. Moore, *J. Am. Chem. Soc.*, 1997, **119**, 10401–10412.
33 F. C. Pigge, M. D. Burgard and N. P. Rath, *Cryst. Growth Des.*, 2003, **3**, 331–337.
34 M. A. S. Aquino, *Coord. Chem. Rev.*, 1998, **170**, 141–202.
35 K. Dunlop, R. Wang, T. S. Cameron and M. A. S. Aquino, *J. Mol. Struct.*, 2014, **1058**, 122–129.
36 Similarly attempts to prepare [Ag_2(**2c**)] under solvothermal conditions were unsuccessful.
37 F. Zhang, S. A. Baudron and M. W. Hosseini, *CrystEngComm*, 2017, **19**, 4393–4400.
38 A. Mazel, S. A. Baudron and M. W. Hosseini, *CrystEngComm*, 2017, **19**, 897–900.
39 C. S. Hawes, K. Byrne, W. Schmitt and T. Gunnlaugsson, *Inorg. Chem.*, 2016, **55**, 11570–11582.
40 C. A. Hollis, S. R. Batten and C. J. Sumby, *Cryst. Growth Des.*, 2013, **13**, 2350–2361.